Supplementary Information for

$K_{Na}1.1$ Gain-of-function Preferentially Dampens Excitability of Murine Parvalbumin-positive Interneurons

Tracy S. Gertler, Suraj Cherian, Jean-Marc DeKeyser, Jennifer Kearney, and Alfred L. George, Jr.

This PDF file includes:

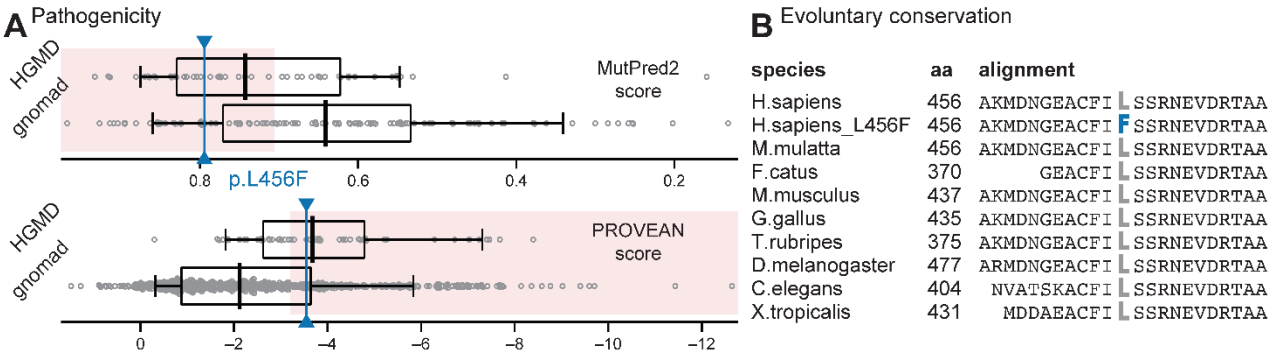

Fig. S1. $K_{Na}1.1$-L456F is predicted to be pathogenic by *in silico* classification algorithms. (**A**) Mutpred2 (0.799 due to altered ordered interface and altered metal binding, threshold of 0.68) and PROVEAN (-3.746, classified deleterious if <-2.5). (**B**) Alignment of $K_{Na}1.1$ amino acid sequences from various species showing leucine at position 456 in human $K_{Na}1.1$ is evolutionarily conserved.

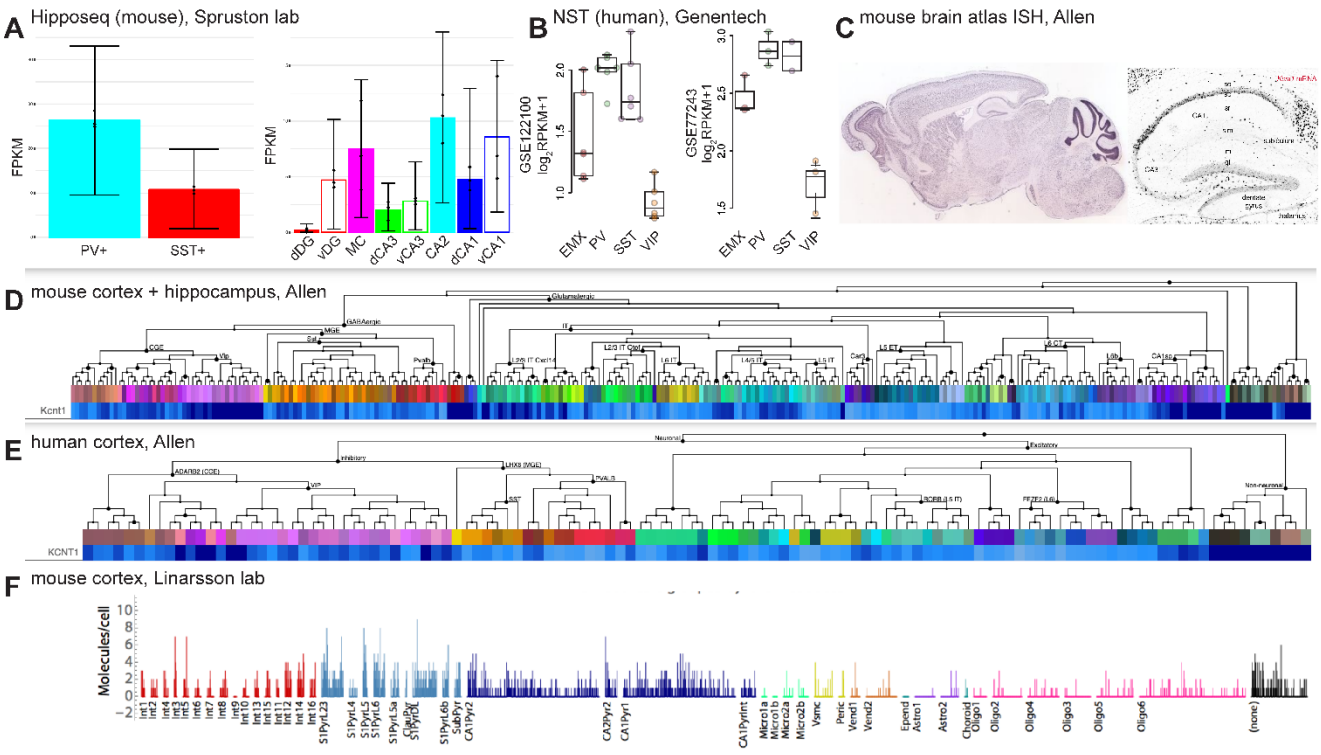

Fig. S2. *Kcnt1* expression is relatively higher in PV+ interneurons compared to other interneuron and principal neuron subclasses. (**A**) An RNA-seq atlas of cells within the hippocampus (1) whereby transgenic mice (P25-P32) with fluorescently-labeled cell subsets from transgenic mice (P25-P32) were microdissected and manually sorted prior to RNA isolation shows relatively higher expression levels in parvalbumin (PV)+ interneurons rather than somatostatin (SST)+ interneurons. In a separate set of experiments, highest expression was seen in the mossy cells (MC) and ventral CA1 (vCA1) pyramidal neurons compared to dentate gyrus (DG) and other dorsal and ventral hippocampal subfields. Values are expressed as Fragments Per Kilobase of Exon Per Million Reads Mapped (FPKM). (**B**) Total RNA sequencing of cells isolated using fluorescence-activated cell sorting from transgenic fluorescence reporter lines (Thy1-GFP lines, EMX-Cre, PV-Cre, VIP-IRES-Cre, SST-IRES-Cre), dissected from either the mouse cortex and hippocampus (GSE122100) and the mouse visual cortex (GSE77243) suggests relatively higher expression of *Kcnt1* within PV+ neurons (2). (**C**) *In situ* hybridization for *Kcnt1* from mouse brains shows a sparse labeling pattern in the hippocampus outside of the pyramidal layer, suggestive of a predominant interneuron expression (3). (**D-E**) Dendrogram and heat maps of single cell RNA-seq data from the Allen brain Institute shows variable *Kcnt1* expression varies by cell subtype in the mouse and human brain. (**f**) *Kcnt1* expression across different cell types assessed by RNA-seq from the Linarsson lab (4) shows predominantly neuronal expression, yet high variability between cells.

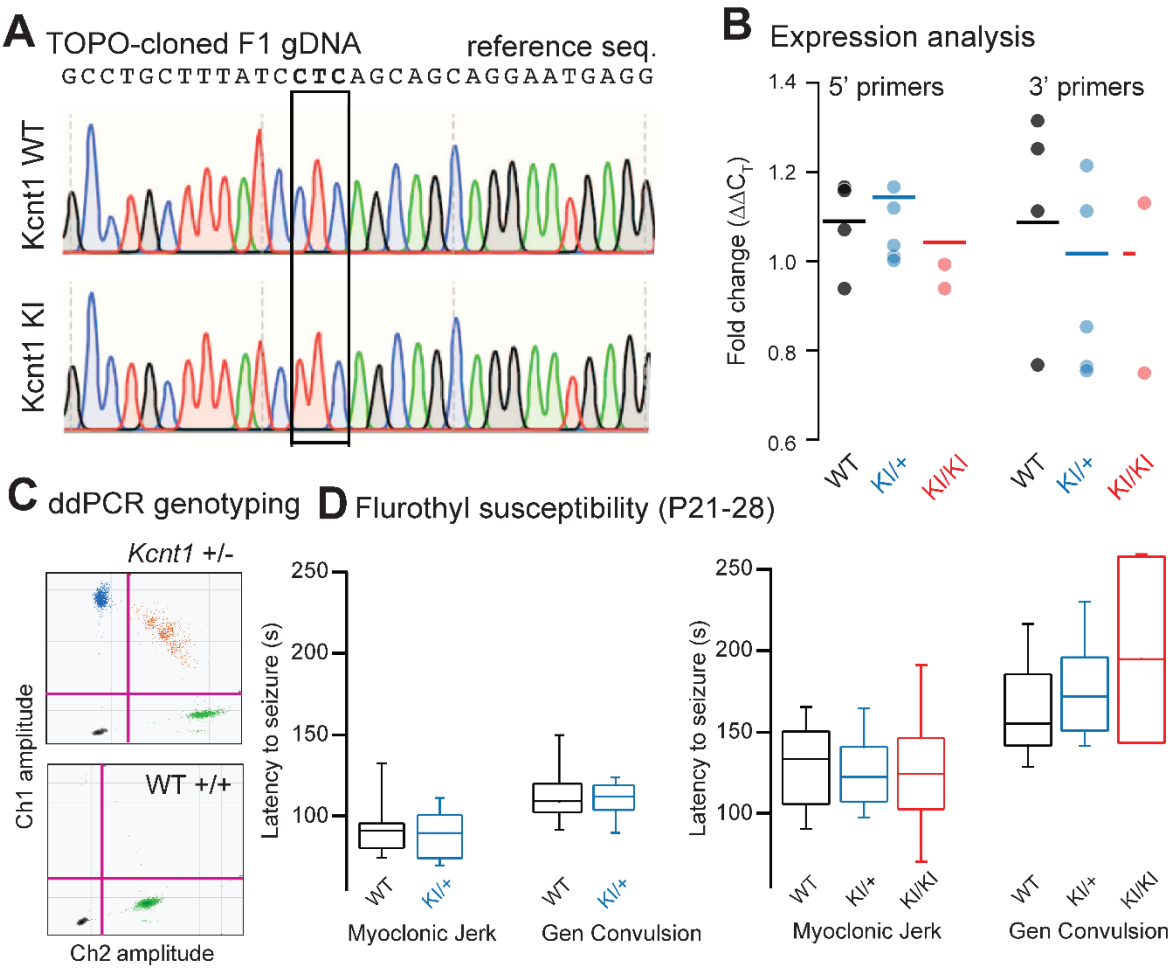

Fig. S3. Genotyping, expression and seizure susceptibility testing of *Kcnt1* knock-in mice. (**A**) Chromatogram of tail DNA from CRISPR-edited *Kcnt1* mouse lines, subcloned to facilitate single allele sequencing. Wild-type CTC codon is aligned with edited TTC codon in knock-in mice. (**B**) Real-time quantitative PCR was performed using primers both upstream and downstream of the editing site to assess changes in transcript levels in each mouse line shows no difference at the 5' end (one-way ANOVA, p = 0.30) or at the 3' end (one-way ANOVA, p = 0.52) (**C**) Digital droplet PCR scatter plot demonstrating clear separation of fluorophore-bound probes in two assays to distinguish wild-type vs knock-in alleles. (**D**) Latency to onset of myoclonic jerk and generalized convulsion with exposure to volatile flurothyl did not show differences in seizure susceptibility at 3 weeks and 6 weeks of age.

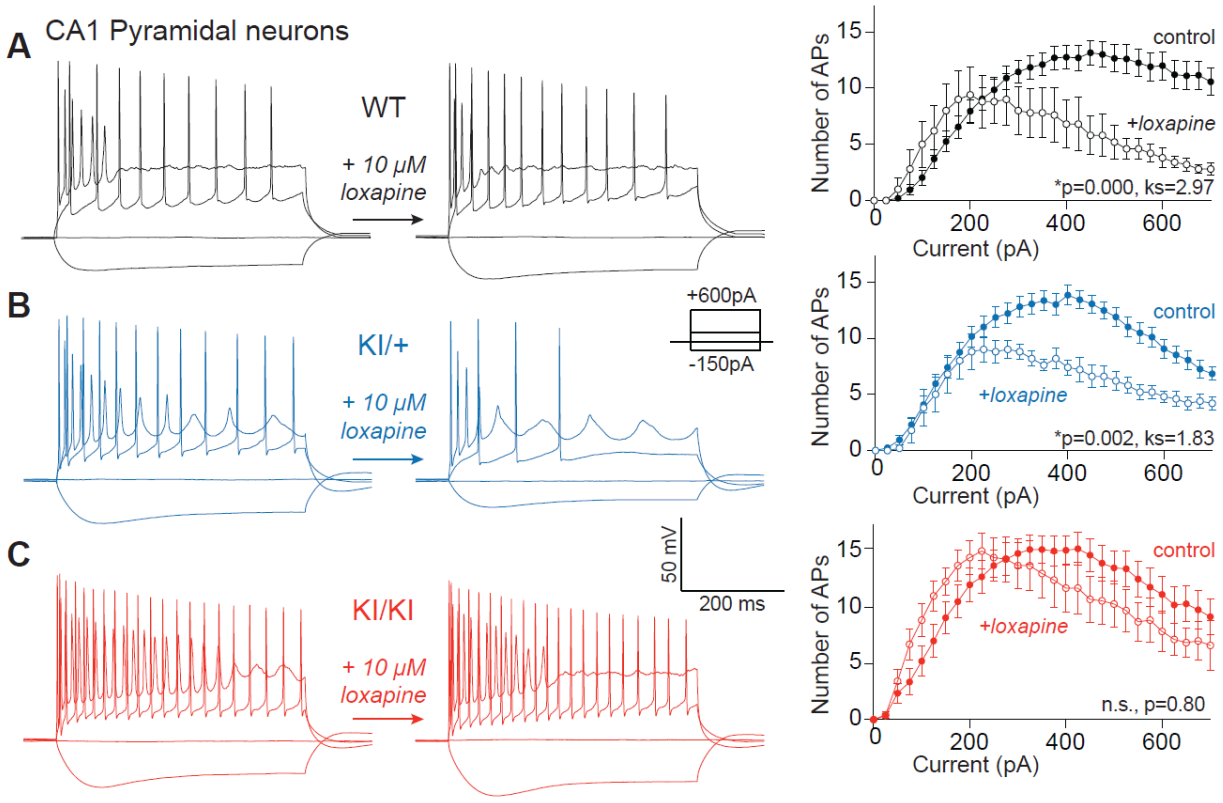

Fig. S4. Loxapine effects on CA1 pyramidal neurons from WT, KI/+ and KI/KI mice. Current clamp recordings from WT (**A**), KI/+ (**B**), and KI/KI (**C**) CA1 pyramidal neurons before and after exposure to 10 μM loxapine. Inset shows voltage protocol. Plots to the right of panels **A**-**C** show comparisons of number of action potentials vs injected current between control and loxapine treated neurons for WT (**A**, control, n= 20; loxapine, n=5), KI/+ (**B**, control, n=20; loxapine, n=5), and KI/KI (**C**, control, n=15; loxapine, n=7). The F-I relationships were significantly different between control and loxapine treated groups for WT and KI/+ neurons but not for KI/KI neurons (Kolmogorov-Smirnov test).

Table S1: Summary of intrinsic electrophysiological properties of CA1 pyramidal neurons in WT, KI/+, and KI/KI mice (values are mean ± SEM).

	WT	KI/+	KI/KI	WT 10uM lox	KI/+ 10uM lox	KI/KI 10uM lox
Rheobase (pA)	118.4 ± 10.7	95 ± 12.2	87.5 ± 13.8	80.0 ± 10.5	90.0 ±s14.2	53.6 ± 10.9
Threshold (mV)	-48.5 ± 0.9	-48.4 ± 0.6	-47.9 ± 0.8	-48.0 ± 2.2	-46.3 ± 1.0	-50.4 ± 1.4
Capacitance (pF)	120.5 ± 7.3	117.4 ± 8.2	109.2 ± 7.0	-	-	-
Input Resistance (MΩ)	68.0 ± 5.0	70.9 ± 4.1	78.3 ± 4.1	82.3 ± 5.6	70.3 ± 12.6	76.8 ± 11.4
Resting potential (mV)	-73.1 ± 0.8	-70.4 ± 1.5	-69.4 ± 1.3	-68.45 ± 1.8	-70.9 ± 1.2	-66.8 ± 1.6
Max current (pA)	448.7 ± 29.1	342.5 ± 20.6	419.64 ± 38.2	255.0 ± 42.8	305.0 ± 47.9	242.9 ± 31.6
Max firing (Hz)	30.2 ± 1.9	29.5 ± 1.4	34.3 ± 2.5	21.2 ± 5.6	21.6 ± 1.9	33.1 ± 2.9
FWHM/Spike width (msec)	1.8 ± 0.04	1.8 ± 0.03	1.8 ± 0.05	1.8 ± 0.08	1.7 ± 0.08	1.6 ± 0.03
Sag Ratio	0.8 ± 0.01	0.78 ± 0.01	0.8 ± 0.01	0.76 ± 0.01	0.73 ± 0.01	0.74 ± 0.01
Spike Height (mV)	96.5 ± 0.9	93.9 ± 1.3	95.5 ± 1.6	94.9 ± 2.7	94.0 ± 1.7	95.1 ± 2.0

p-values **(Mann-Whitney test)**

	WT vs KI/+	WT vs KI/KI	WT vs WT (lox)	KI/+ vs KI/+ (lox)	KI/KI vs KI/KI (lox)
Rheobase (pA)	0.100	0.092	0.060	0.948	0.153
Threshold (mV)	0.967	0.957	0.891	0.169	0.128
Capacitance (pF)	0.550	0.298	-	-	-
Input Resistance (MΩ)	0.428	0.065	**0.036**	0.818	0.971
Resting potential (mV)	**0.038**	**0.032**	**0.019**	0.717	0.224
Max current (pA)	**0.004**	0.464	**0.004**	0.457	**0.001**
Max firing (Hz)	0.861	0.188	0.133	**0.008**	0.620
FWHM/Spike width (msec)	0.945	0.461	0.629	0.668	**0.012**
Sag Ratio	0.204	0.267	0.103	**0.042**	**0.001**
Spike Height (mV)	0.079	0.733	0.534	0.921	0.913

Table S2: Summary of intrinsic electrophysiological properties of PV+ interneurons in WT, KI/+, and KI/KI mice (values are mean ± SEM; lox, loxapine)

	WT	KI/+	WT 10μM lox	KI/+ 10μM lox
Rheobase (pA)	173.7 ± 19.0	186.9 ± 30.1	167.9 ± 41.8	162.5 ± 31.7
Threshold (mV)	-47.2 ± 1.3	-45.0 ± 1.0	-48.2 ± 1.0	-43.6 ± 3.1
Capacitance (pF)	83.6 ± 8.4	79.5 ± 7.1	-	-
Input Resistance (MΩ)	75.5 ± 7.0	72.5 ± 5.6	78.7 ± 15.4	89.2 ± 12.8
Resting potential (mV)	-66.8 ± 1.1	-65.6 ± 1.0	-69.2 ± 2.1	-66.5 ± 0.6
Max current (pA)	1230.3 ± 93.9	1106.0 ± 116.6	1014.3 ± 113.9	796.9 ± 143.8
Max firing (Hz)	148.3 ± 5.4	135.4 ± 7.4	120.9 ± 6.2	110.5 ± 15.7
FWHM/Spike width (msec)	0.69 ± 0.02	0.73 ± 0.03	0.68 ± 0.03	0.73 ± 0.04
Sag Ratio	0.92 ± 0.01	0.91 ± 0.01	0.84 ± 0.08	0.93 ± 0.01
Spike Height (mV)	64.4 ± 1.2	62.0 ± 2.0	64.7 ± 2.9	61.4 ± 2.7

p-values (Mann-Whitney test)

	WT vs KI/+	WT vs WT (lox)	KI/+ vs KI/+ (lox)
Rheobase (pA)	0.856	0.831	0.492
Threshold (mV)	0.134	0.866	0.462
Capacitance (pF)	0.732	-	-
Input Resistance (MΩ)	0.893	1.000	0.253
Resting potential (mV)	0.531	0.209	0.108
Max current (pA)	0.409	0.139	0.100
Max firing (Hz)	0.285	**0.010**	0.142
FWHM/Spike width (msec)	0.507	0.866	0.511
Sag Ratio	0.555	0.701	0.712
Spike Height (mV)	0.376	0.651	0.543

SUPPLEMENTARY REFERENCES

1. M. S. Cembrowski, L. Wang, K. Sugino, B. C. Shields, N. Spruston, Hipposeq: a comprehensive RNA-seq database of gene expression in hippocampal principal neurons. *Elife* **5**, e14997 (2016).
2. M. A. Huntley *et al.*, Genome-Wide Analysis of Differential Gene Expression and Splicing in Excitatory Neurons and Interneuron Subtypes. *J Neurosci* **40**, 958-973 (2020).
3. J. D. Hahn *et al.*, An open access mouse brain flatmap and upgraded rat and human brain flatmaps based on current reference atlases. *J Comp Neurol* **529**, 576-594 (2021).
4. A. Zeisel *et al.*, Brain structure. Cell types in the mouse cortex and hippocampus revealed by single-cell RNA-seq. *Science* **347**, 1138-1142 (2015).